Available online at www.sciencedirect.com
ScienceDirect
Physica D 224 (2006) 202–212
PHYSICA D
www.elsevier.com/locate/physd

Structural and functional clusters of complex brain networks

Lucia Zemanová*, Changsong Zhou, Jürgen Kurths

Institute of Physics, University of Potsdam, PF 601553, 14415 Potsdam, Germany

Available online 2 November 2006
Communicated by A. Doelman

Abstract

Recent research using the complex network approach has revealed a rich and complicated network topology in the cortical connectivity of mammalian brains. It is of importance to understand the implications of such complex network structures in the functional organization of the brain activities. Here we study this problem from the viewpoint of dynamical complex networks. We investigate synchronization dynamics on the corticocortical network of the cat by modeling each node (cortical area) of the network with a sub-network of interacting excitable neurons. We find that the network displays clustered synchronization behavior, and the dynamical clusters coincide with the topological community structures observed in the anatomical network. Our results provide insights into the relationship between the global organization and the functional specialization of the brain cortex.

Keywords: Cortical network; Anatomical connectivity; Functional connectivity; Topological community; Dynamical cluster

1. Introduction

Real-world complex systems are composed of interacting entities with nontrivial dynamical behavior and complicated interaction topology. Over the years, the complex network approach has been playing an increasing role in the study of complex systems [1–4]. The main research focus has been on the topological structures of complex systems based on simplified graphs, paying special attention to the global properties of complex networks, such as the scale-free and small-world features, or to the presence or absence of some very small subgraphs, such as network motifs [5]. The topological studies have revealed important organization principles in the structures of many realistic network systems [1–4]. Recently, significant research interests have been shifted to understanding the dynamics of such network systems beyond the interaction topology (for a recent review see Ref. [4]). A problem of fundamental importance is the impact of topological structures on the dynamics of the networks. For example, synchronization of oscillators [6–11] is one of the crucial dynamical behaviors on complex networks, for its relevance in various fields, especially in neural systems.

A mammalian brain is a complex system consisting of a hierarchy of interacting elements on different levels, of different functions and different interconnections. There are at least three basic levels in the hierarchical structure: the microscopic level of interacting neurons, mesoscopic level of mini-columns and local neural circuits, and macroscopic level of large-scale organization of the brain areas [12–14]. The complex network approach has been widely applied to obtain information about the segregation and the integration of different brain parts. Neural network structures on various levels are found to display properties of many other complex networks, such as high clustering coefficient and short average pathlength. Especially, significant progress has been made in the study of the large-scale organization of the corticocortical connections in the brain of animals, like cat and macaque monkey [15,16]. The topological properties of human connectome, however, remain largely unclear [14]. The *anatomical connectivity* of the animal brain displays features of small-world and scale-free networks [16], and organizes into clusters (communities) [17,18].

It is known that different areas of the brain cortex are functionally correlated, which is manifested by interdependence

* Corresponding author. Tel.: +49 331 9771431; fax: +49 331 9771142.
E-mail addresses: zemanova@agnld.uni-potsdam.de (L. Zemanová), cszhou@agnld.uni-potsdam.de (C. Zhou).

0167-2789/$ - see front matter © 2006 Elsevier B.V. All rights reserved.
doi:10.1016/j.physd.2006.09.008

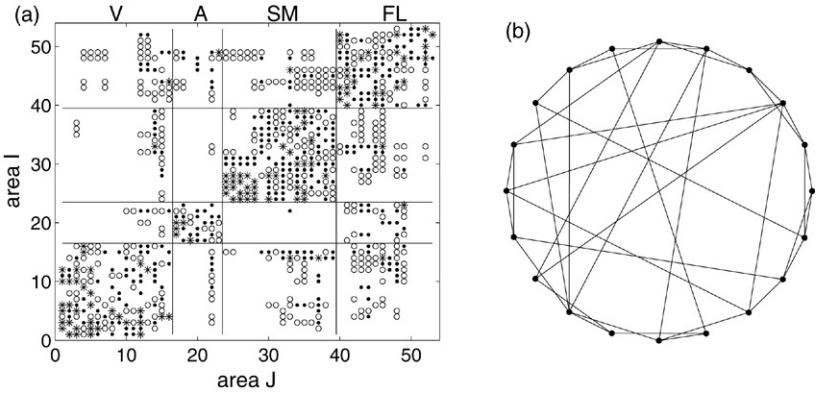

Fig. 1. (a) Connection matrix M^C of the cortical network of the cat brain. A symbol at the entry $M^C(I, J)$ indicates an afferent connection to the area I from the area J. The different symbols represent different level of the connection weight: 1 (•sparse), 2 (∘ intermediate) and 3 (∗ dense). The organization of the system into four topological communities (functional sub-systems, V, A, SM, FL) is indicated by the solid lines. (b) The small-world sub-network (schematic plot) used to model each node of the cat cortical network in (a).

and synchronization of the dynamical activities of different areas [16]. The network approach has been also applied to investigate the organization of the *functional connectivity* based on large-scale measurement of brain activities [19–22]. Interestingly, the functional brain networks also exhibit basic properties of small-world and scale-free networks.

In spite of the progress made in revealing the general principles of structural and functional networks, the relationship between these two parts is still an open problem and a big challenge requiring significant development in various fields ranging from neurobiology to complex system theory. A complete understanding of this problem would involve detailed information about the hierarchical structures of the anatomical and functional connectivities. Unfortunately, such detailed information crossing various hierarchies is still largely not available, and research has to mainly focus on certain levels separately. This, however, does not prevent us from accessing the problem from the viewpoint of dynamical complex network systems. Conceptual modeling of the dynamics of the neural system based on a realistic network of corticocortical connections and investigating the synchronization behavior should provide meaningful insight into the problem.

In this paper, we simulate the functional connectivity by modeling each node of the cat cortical network [12] with a sub-network of interacting FitzHugh–Nagumo (FHN) excitable neurons in the presence of noise. The functional connectivity among the cortical areas is measured by the correlation between the mean activities of the sub-networks. We will study different regimes of synchronization in the networks. We will analyze the clustering behavior of the dynamical patterns and study their relationship with the underlying anatomical structures of the network. Our main finding is that in the biologically plausible regime, the dynamical clusters reveal the topological communities of the anatomical network.

The paper is organized as follows. In Section 2 we present an introduction of the cat corticocortical network and our dynamical model. The overall dynamical properties of the model are discussed in Section 3. We then study in detail cluster formations in Section 4. In Section 5, we compare the cat cortical network with randomized networks and demonstrate different mechanisms of synchronization organization. Section 6 is devoted to discussion and outlook.

2. Dynamical neural network model

2.1. Corticocortical network of cat

The corticocortical network that we study in this paper represents the long-range projections between cortical areas in mammalian brains. For the cat brain, the cortex can be divided into 53 areas from four major systems: 16 areas in the visual system (V), 7 areas in the auditory part (A), 16 areas in the somato-motor (SM) and 14 areas in the fronto-limbic system (FL). The connectivity between these areas was identified by collating data from various anatomical tracer studies [12]. The 53 areas in the cat cortical network are linked with approximately 830 fiber connections. The fibers connecting the areas have different axon densities, and the sparse connections are weighted as 1, dense connections as 3 and intermediate or unknown density are labeled as 2. This gives rise to a weighted complex network, as shown in Fig. 1(a).

The complex topology of cortical networks is the subject of many recent analyses, see Ref. [16] for a recent review. The cat network displays typical small-world properties, i.e., short average pathlength and high clustering coefficient, indicating optimal organization for effective inter-area communication and for achieving high functional complexity [15,18]. The degree (the number of connections) of the nodes is heterogeneous, for example, some nodes have only 2–3 links, while some others have up to 32 connections. Due to the small number of areas it is difficult to claim a scale-free degree distribution [18], nevertheless, our analysis comparing the cat cortical network to a scale-free network model with the same size and connectivity density does suggest a scale-free degree distribution [23].

Hilgetag et al. have analyzed the cluster organization of the cat cortical network using an evolutionary optimization algorithm [17,18]. The clusters have been identified based on the rationale that clustered areas should be more densely connected within the respective clusters than with areas in

other clusters. Maximizing the intra-cluster connections and minimizing the inter-cluster ones with this optimization scheme identifies a small number of clusters. Interestingly, these topological clusters agree broadly with the four functional cortical sub-divisions, i.e., the V, A, SM and FL systems. We note that this way of defining clusters in Refs. [17,18] is essentially the same as the modularity measure used to find network communities [24]. Because the network communities based on the connectivity topology coincide with the functional sub-systems, we will give these topological communities the corresponding names of the cortical sub-systems V, A, SM and FL to contrast them from the dynamical clusters.

Our following analysis of the dynamics of this network shows that the dynamical patterns are also clustered, and strikingly, in the biologically plausible regime, the dynamical clusters also coincide with the anatomical communities and the functional sub-divisions V, A, SM and FL. Our finding thus provides a dynamical link between the topological structure and functional specialization of brain networks.

2.2. Dynamical model

Each node of the cat cortical network corresponds to a cortical area composed of a large ensemble of interacting neurons. However, detailed information about the connectivity at the neuronal level is still largely missing, so we introduce a conceptual model. For the purpose of dynamical modeling, we represent each node (area) of the cat cortical network with a sub-network of N_a interacting neurons. These neurons are coupled with the small-world network (SWN) model proposed in Ref. [3], i.e., a regular array of N neurons with a mean degree k_a is rewired with a probability p, as depicted in Fig. 1(b). In spite of its simplicity, such a model incorporates the basic features of neuronal networks in the local area of the cortex, i.e., neurons are mainly connected to their spatial neighbors, but also with some additional distant synapses. Much previous work has studied synchronization in SWNs of neurons [8–11], and has found that SWNs enhance the ability of the system to synchronize. In our investigation of the dynamical organization of the cat cortical network at the systems level, we do not pay special attention to the detailed synchronization behavior of the sub-network, but mainly consider the correlations of mean activity between the sub-networks. Reflecting biological observations, 25% of the N_a neurons are set as inhibitory neurons, with the rest being excitatory. It has been observed that only a small number of neurons (about 5%) of one area receive excitatory synapses from another connected area [25]. To our knowledge, no information about the output synapses is available, and for simplicity, we assume that the output signal from one area to another area is the mean activity of the output area.

Specifically, our model of the neural network of cat cortex is composed of a large ensemble of neurons connected in a *network of networks*, and the dynamics of the neuron i at area I is:

$$\epsilon \dot{x}_{I,i} = f(x_{I,i}) + \frac{g_1}{k_a}\sum_{j}^{N_a} M_I^L(i,j)(x_{I,j} - x_{I,i}) + \frac{g_2}{\langle w\rangle}\sum_{J}^{N} M^C(I,J)L_{I,J}(i)(\bar{x}_J - x_{I,i}), \quad (1)$$

$$\dot{y}_{I,i} = x_{I,i} + a_{I,i} + D\xi_{I,i}(t), \quad (2)$$

where

$$f(x_{I,i}) = x_{I,i} - \frac{x_{I,i}^3}{3} - y_{I,i}. \quad (3)$$

Here, the matrix M^C represents the corticocortical connections in the cat network ($M^C(I,J)$: $I,J = 1,\ldots,N = 53$). M_I^L denotes the local SWN of the Ith area ($M_I^L(i,j)$: $i,j = 1,\ldots,N_a$). A neuron j is inhibitory if $M_I^L(i,j) = -1$ for all of its connected neighbors. The label $L_{I,J}(i) = 1$ if the neuron i is among the 5% within the area I receiving the mean-field signal $\bar{x}_J = (1/N)\sum_l^{N_a} x_{J,l}$ from the area J, otherwise, $L_{I,J}(i) = 0$. The coupling strength normalized by the mean degree k_a of the SWNs, g_1, corresponds to the amount of internal interactions within one area. The strength of the external interaction between areas, g_2, is normalized by the average weight of connection ($\langle w\rangle \approx 2$).

We use the FHN model [26] for the dynamics of individual neurons, mainly because of its simplicity and biological plausibility [27]. The fast variable x ($\epsilon = 0.01$ in Eq. (1)) denotes the membrane potential and the slow variable y describes a recovery of the dynamics. The FHN equations model class II excitable neurons, which are characterized by a Hopf bifurcation from the excitable regime to an oscillatory regime. In our modeling, all the neurons are set in the excitable regime with the parameters $a_{I,i} > 1$. To take into account the non-identity of the neurons, a is randomly and uniformly distributed in the interval $a \in (1.05, 1.15)$. Additionally, independent Gaussian white noise $\langle \xi_{I,i}(t)\xi_{J,j}(t-\tau)\rangle = \delta_{I,J}\delta_{ij}\delta(\tau)$ with an intensity $D = 0.03$ is added to each neuron in order to simulate perturbations, e.g., from subcortical areas. For isolated neurons, the noise can generate sparse, Poisson-like irregular spiking patterns as in realistic neurons. Diffusive coupling is mainly considered to represent the electrical interaction between neurons for the simplicity of simulation at this stage, although it is not the most typical manifestation found in the mammalian cortex. More realistic interactions through chemical synapses will be studied in ongoing work.

3. General dynamics of the model

The above system of Eqs. (1)–(3), the network of networks of neurons, is simulated using the first order Euler algorithm with a time step $\Delta t = 0.001$, which is sufficiently small for the stochastic dynamics. To keep the simulation time reasonable, we fix the small-world sub-networks with $N_a = 200$, $k_a = 12$ and $p = 0.3$. We have checked that $N_a = 200$ is large enough to exclude the system size effects on the amplitudes of the mean field $\bar{x}$ of the individual SWNs without external coupling ($g_2 = 0$).

For a fixed input noise level D, the spiking dynamics and the synchronization of the neurons in the SWNs are mainly

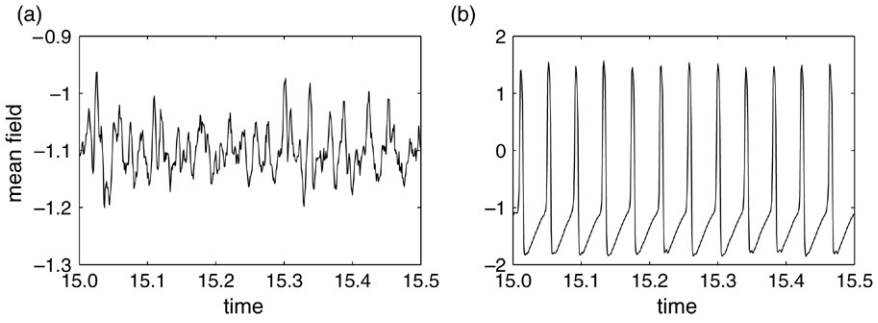

Fig. 2. Typical time series of the mean field dynamics $\bar{x}$ of one area with different internal coupling strengths $g_1 = 0.06$ (a) and $g_1 = 0.12$ (b). Notice the different scales on the vertical axes.

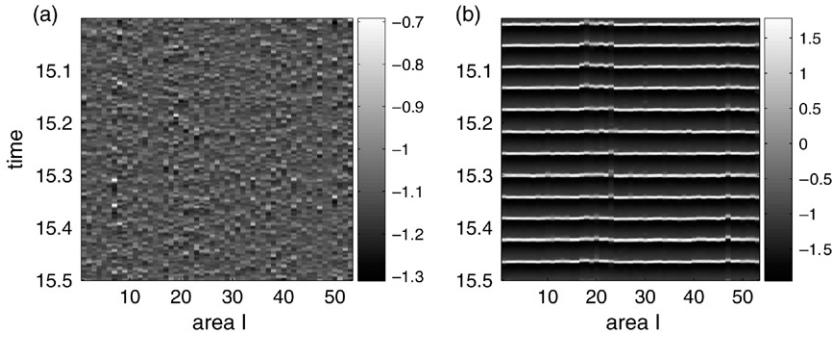

Fig. 3. Spatio-temporal patterns of the mean activity $\bar{x}_I$ at different coupling strengths: (a) $g_1 = 0.06$, $g_2 = 0.12$ and (b) $g_1 = 0.12$, $g_2 = 0.12$. Note the different gray-scales in the colorbars.

controlled by the internal coupling g_1 [28]. For small g_1, a neuron is not often excited by the noise-induced spiking of its connected neighbors, and the mean field $\bar{x}$ displays irregular fluctuations. Weak synchronization in the SWNs is manifested by some clear deviations of $\bar{x}$ from the baseline (Fig. 2(a)). However, for large enough g_1, the neurons are excited mutually and achieve strongly synchronized and regular spiking behavior, as illustrated by the time series of $\bar{x}$ in Fig. 2(b). The external coupling g_2 also has an effect on the synchronization of the local network (amplitudes of $\bar{x}$), as well as controlling the synchronization between the areas. For small g_1, the infrequent and irregular spiking activity of one area does not very much affect the behavior of the other connected areas, and the correlations between the areas are not strong even for significantly large g_2, mainly due to the fact that only 5% of the neurons are receiving signals from another connected area. At large values of g_1, the frequent and regular spiking activity of one area has significant effects on the spike timing of the other connected areas, and the whole network exhibits strong synchronization even for relatively small g_2. Fig. 3 illustrates the typical behavior in these two regimes. We can observe some weakly synchronized activities among certain areas in Fig. 3(a) and some temporal interruption of the strong synchronization at some other areas in Fig. 3(b). The infrequent spiking and weak synchronization regime is biological plausible, like in normal brain activity, and the regular spiking and strong synchronization regime could correspond to pathological situations, such as epileptic seizure [29].

To measure the degree of synchronization among the stochastic signals of the mean field activities $\bar{x}_I$, we compute

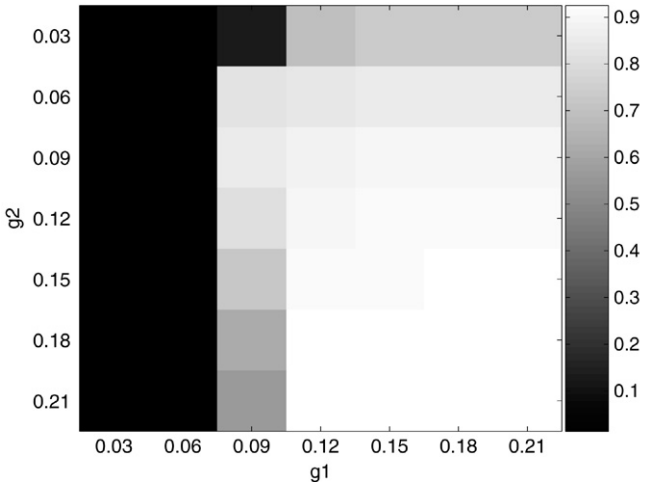

Fig. 4. Dependence of the average correlation coefficient R on the internal and external coupling strength g_1 and g_2.

the correlation coefficient between the areas using long time series after the transient, namely,

$$r(I, J) = \frac{\langle \bar{x}_I \bar{x}_J \rangle - \langle \bar{x}_I \rangle \langle \bar{x}_J \rangle}{\sigma(\bar{x}_I)\sigma(\bar{x}_J)}, \tag{4}$$

where $\langle \cdot \rangle$ denotes averaging over time.

First, we quantify the level of synchronization of the whole network system by computing the average correlation coefficient over all the $N(N-1)$ pairs of areas, $R = [1/(N(N-1))] \sum_{I \neq J} r(I, J)$. A plot of R as a function of the coupling strengths g_1 and g_2 is shown in Fig. 4. Here, the results

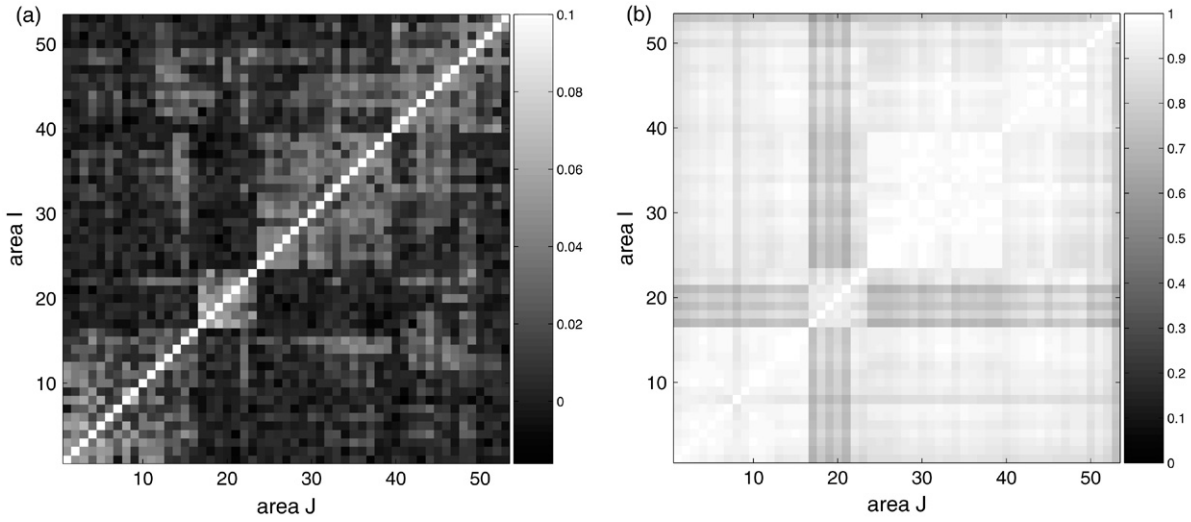

Fig. 5. Correlation matrices $r(I, J)$ corresponding to the spatio-temporal patterns in Fig. 3. (a) $g_1 = 0.06$, $g_2 = 0.12$ and (b) $g_1 = 0.12$, $g_2 = 0.12$. Note the different gray-scales in the colorbars.

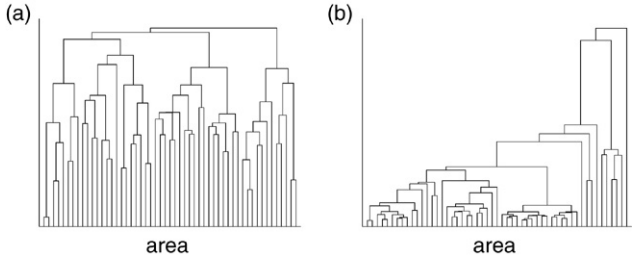

Fig. 6. Graphical representation of cluster hierarchy (dendrogram) in both synchronization regimes. (a) $g_1 = 0.06$, $g_2 = 0.12$ and (b) $g_1 = 0.12$, $g_2 = 0.12$.

are averaged over 10 realizations of the sub-networks and initial conditions for each set of the parameters. As already discussed, an increase of the coupling strengths g_1 leads to stronger interaction of the neurons and to a rapid growth of their synchronous activity within and across areas for non-vanishing g_2. In the region with an intermediate internal coupling strength g_1 (e.g., $g_1 = 0.09$) the transition from a very low to a high degree of correlation is evident with increasing g_2.

The patterns of the correlation matrix $r(I, J)$ for the two representative regimes of weak and strong synchronization are shown in Fig. 5(a) and (b) respectively. Although the average levels of synchronization (R) are very different, both of the correlation patterns display some dynamical clusters, where a dynamical (functional) cluster is defined as a group of the brain areas communicating much more strongly within this set than with the areas in the rest of the brain [30]. In our case, these clusters are also seen in the spatio-temporal patterns in Fig. 3.

4. Cluster analysis

In the following section, we investigate the structure of the correlation matrix by using cluster analysis and discuss the relationship of the resulting clusters to the anatomy of the network.

As mentioned above, in the original matrix of the cat cortical network, the anatomical connections create specific communities consistent with the functional sub-systems V, A, SM and FL. To analyze the dynamical clusters, we calculate the dissimilarity matrix $d = [d(I, J) = 1 - r(I, J)]$ and apply a hierarchical clustering algorithm to create a cluster tree [31] (using the Statistics Toolbox in Matlab, version 7.0.1). Typical hierarchy of the clusters (dendrogram) is shown in Fig. 6(a) and (b) for the weak and strong synchronization regimes.

In order to compare the anatomy with the correlation clusters, we concentrate on the level in the hierarchy of the cluster where the correlation matrix decomposes into the number of clusters (here 4), corresponding to the number of anatomical communities.

On this level the cluster formation in the weak and the strong synchronization regimes is demonstrated and described in detail.

4.1. Weak synchronization regime

In the weak synchronization regime, neurons fire with low frequencies characterized by irregular spiking sequences and irregular mean activity (Fig. 2(a)). The mean field signals are similar to those observed experimentally (e.g., EEG data [32]) and thus this regime is not biologically implausible. The integration of areas into the dynamical clusters due to synchronization closely resembles the pattern of communities obtained using the graph theoretical tools based on anatomical structures [17,18]. Typical dynamical clusters for the weak synchronization regimes are shown in Fig. 7. The four dynamical clusters correspond to the functional sub-division of the cortex — C_1 (V), C_2 (A), C_3 (SM), C_4 (FL). However, it is also important to notice that there are a few bridging nodes which belong to one anatomical community but join another dynamical cluster. For example, the area $I = 49$ (anatomically named as 36 in the cat cortex) of the fronto-limbic system is in the dynamical cluster C_2, which is mainly composed of areas from the auditory system (Fig. 7 (C_2)). A detailed inspection reveals that these nodes are the areas sitting in one anatomical community but in close connectional association

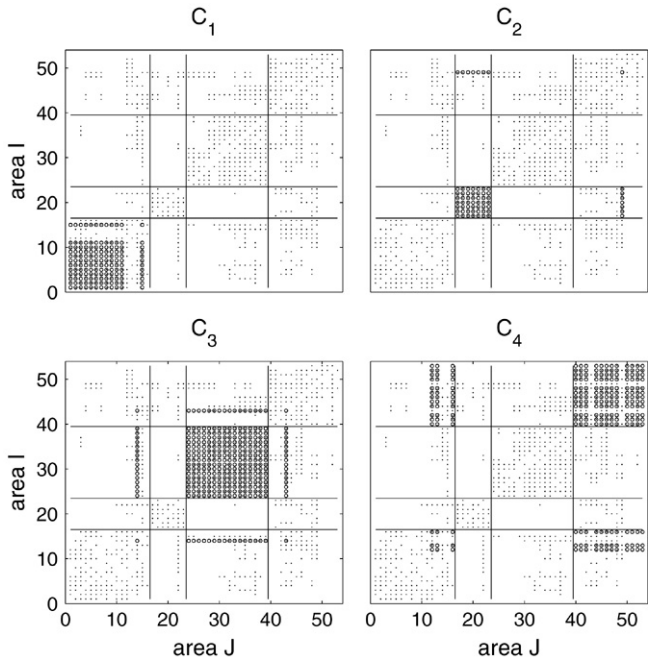

Fig. 7. The four dynamical clusters (constituting correlation pairs indicated by (∘) in the respective panel) obtained at weak internal coupling strength $g_1 = 0.06$ and $g_2 = 0.12$. The underlying anatomical connections are indicated by (·).

with areas in other communities [12]. As displayed in Table 1, we calculate the degree (total number of connections) and the intensity (total weights) of the input connections of these areas from other areas within the respective communities and from other communities. Comparing to the overall connection degrees (intensities) among the four anatomical communities in Table 2, we can see that these few bridging nodes identified in our dynamical clustering analysis take over a significant part of the inter-community connections. In particular, the three areas $I = 12, 13$ and 16 account for about 40% of the afferent connections from FL to V, and dynamically they join the cluster C_4 in Fig. 7.

With variation of the coupling strengths in the weak synchronization regime, we can observe slightly different combinations of such bridging areas. The areas we identified are: $I = 12$ (20a), 13 (20b), 14 (7), 15 (AES), 16 (PS), 22 (EPp), 23 (Tem), 33 (6m), 43 (Ia), 44 (Ig), 46 (CGp) and 49 (36); this list is in strikingly good agreement with all those special areas pointed out previously [12] that may play special roles in the information processing in the brain. Our results suggest that, due to the role of the inter-community association played by these nodes, they are acting as the bridge of communication among the functional communities, in the sense that the dynamics of these nodes integrates the dynamics of different anatomical communities.

To measure in a more quantitative way the coincidence of the dynamical clusters and the anatomical communities, we examine each dynamical cluster and check from which anatomical communities the areas are from. On the other hand, we also examine how the areas of a topological community are involved into different dynamical clusters. The distribution of

Table 1
Input degree (intensity) from the four communities (V, A, SM, FL) to the bridging nodes (identified in Fig. 7) from one topological community (CM) but in another dynamical cluster (CL)

Area(name)	CM(CL)	V	A	SM	FL
12(20a)	V(C_4)	10 (23)	1 (2)	2 (2)	7 (9)
13(20b)	V(C_4)	6 (10)	1 (2)	2 (2)	8 (11)
16(PS)	V(C_4)	10 (15)	0 (0)	0 (0)	6 (8)
14(7)	V(C_3)	6 (8)	1 (2)	9 (18)	7 (10)
43(Ia)	FL(C_3)	5 (5)	3 (4)	9 (10)	8 (16)
49(36)	FL(C_2)	8 (10)	4 (8)	9 (9)	11 (20)

Table 2
Input degree (intensity) of the areas among the four anatomical communities

CM	V	A	SM	FL
V	140 (264)	11 (15)	51 (76)	53 (71)
A	11 (14)	34 (63)	1 (2)	27 (42)
SM	28 (38)	2 (2)	178 (340)	53 (67)
FL	45 (57)	20 (31)	54 (65)	118 (225)

E.g., the community V receives 51 connections from SM.

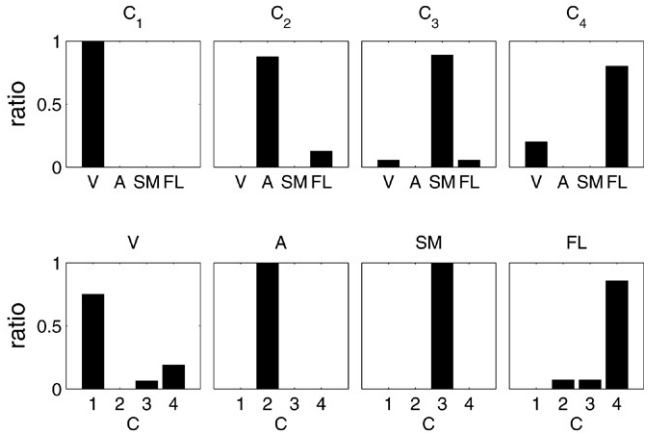

Fig. 8. Upper panel: composition of dynamical clusters from different anatomical communities. Lower panel: participation of the areas in a community into different dynamical clusters. The results correspond to the clusters in Fig. 7.

the dynamical clusters into the anatomical communities and vice versa is summarized in Fig. 8. The agreement between the dynamical clusters and topological communities is clearly seen by a major bar with a ratio ≈1 in the respective histograms.

Our analysis of the dynamical clusters provides a meaningful bridge that mediates the gap between the topology (communities) and function (functional sub-division) of the brain cortex, even though the sub-networks we consider here are strongly simplified and the dynamics does not reflect specific information processing.

4.2. Strong synchronization regime

In the second synchronization regime, typical for stronger internal coupling, the mean field signals of the areas exhibit regular spikes with high amplitude and frequency, which have a higher correlation between the areas. However, this type of

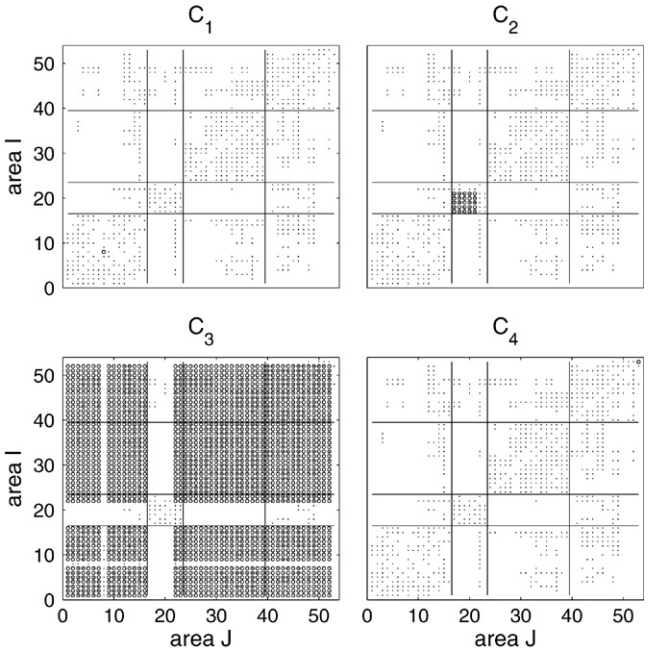

Fig. 9. Dynamical clusters at strong internal coupling strength $g_1 = 0.12$ ($g_2 = 0.12$). C_1 and C_4 contain only a single node, $I = 8$ from V and $I = 53$ from FL, respectively.

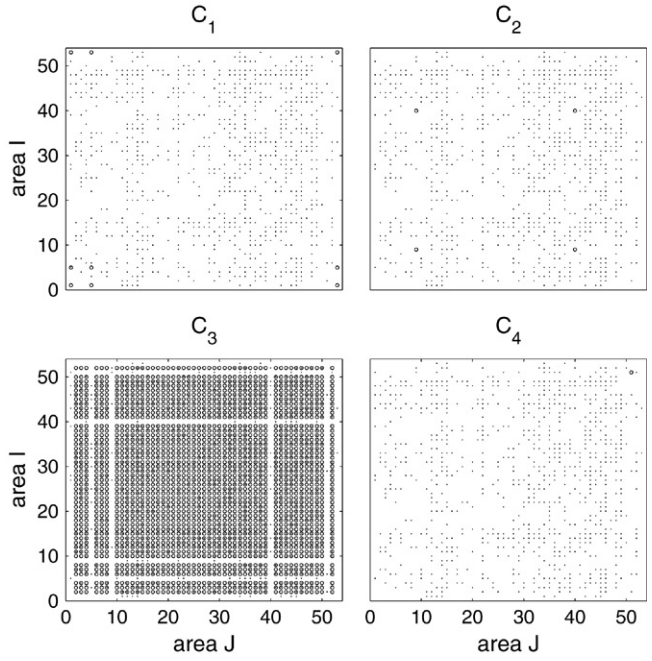

Fig. 10. Dynamical clusters (∘) with weak internal coupling strength $g_1 = 0.06$ ($g_2 = 0.12$), compared to the underlying random connections (·).

clustering dynamics is mainly characterized by two dominant clusters that contain the majority of nodes, with a few single areas as separate clusters (Fig. 9). When the coupling strength g_1 is increased (e.g., from 0.08 to 0.09), the three dynamical clusters corresponding to the major parts of the V, SM and FL communities as in Fig. 7 (C_1, C_3, C_4) merge to give rise to a large cluster containing most of the nodes of the network (Fig. 9 (C_3)). The community SM plays a crucial role in the formation of this large dynamical cluster: by increasing the coupling strength, the cluster expands and absorbs large parts from the V and FL communities due to the strong inter-community connections of the SM community with the latter ones.

We have found that variation of the internal and the external coupling strengths g_1 and g_2 does not much affect the formation of the cluster C_2. This cluster is mainly composed of areas from the auditory system (Fig. 7 (C_2) and Fig. 9 (C_2)) which are strongly (weight = 2–3) and nearly completely connected. Such connectivity provides a reason for the strong stability of the dynamical clustering of these areas both in the weak and strong synchronization regimes, irrespective of the coupling strengths.

There are some areas, different for various parameter combinations, that preserve their independence and form single clusters. These nodes are: $I = 1$ (17), 8 (VLS), 21 (VPc), 23 (Tem), 47 (RS) and 53 (Hipp). The separation of these areas as relatively independent dynamical nodes comes perhaps from their specific biological origin. For example, the exclusion of the hippocampus from the dominant network dynamics can be caused by its distance from the sensory periphery [12].

5. Comparison with random networks

To further understand the different mechanisms of cluster formation in the weak and the strong synchronization regimes, we compare the cat cortical network with corresponding random networks. We apply a rewiring algorithm proposed by Milo et al. [5] to generate random networks (M^R) that preserves the degrees and weights of the incoming connections of the cat cortical network M^C, but destroys any other topological organization. Specifically, two pairs of connected nodes are randomly selected, (x_1, y_1) and (x_2, y_2), and the connections are changed to (x_2, y_1) and (x_1, y_2) if such connections do not exist. This procedure is repeated until the network becomes random. We then repeat the simulations of the dynamics and the analysis of clusters with the randomized matrix M^R for the same sets of parameters as in Figs. 7 and 9. The behavior of the mean activities of the sub-networks and the overall degree of synchronization are very similar to the original cat cortical network (Figs. 2 and 4), but the cluster formation has been changed. As seen in Figs. 10 and 11 with one typical realization of the random networks, for both the weak and the strong synchronization regimes, we have one major cluster and a few other clusters each containing only a few (1–3) nodes. In the strong synchronization regime the auditory cluster (C_2 in Fig. 9) is destroyed; most of these areas join the major cluster in the random networks, since these nodes are no longer strongly connected among themselves. Nevertheless, the major cluster C_3 and the independent single nodes C_1 and C_4 in Fig. 9 remain largely unchanged in the random network (Fig. 11). This suggests that the dynamical organization in the strong synchronization regime is mainly determined by the input degrees and intensities of the nodes, which are the same in the original and in the randomized networks.

The analysis below confirms the dependence of synchronization on the intensities. First, we can assume the following

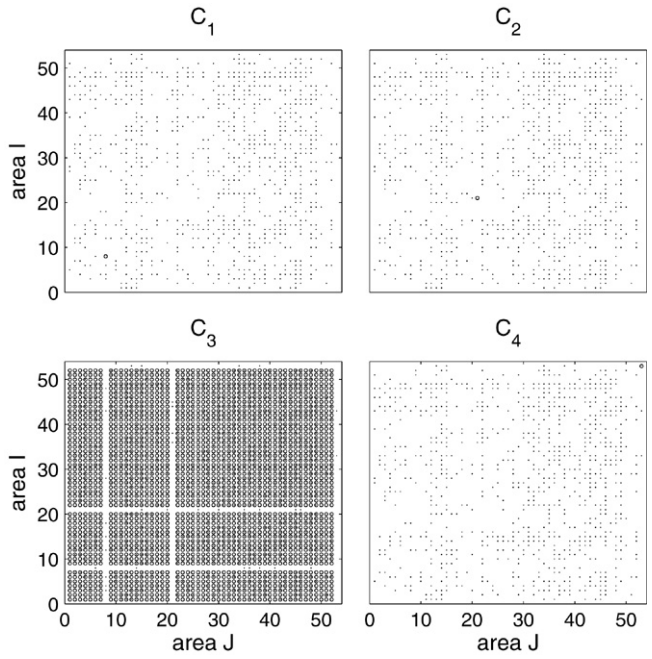

Fig. 11. Dynamical clusters in the random network with strong internal coupling strength $g_1 = 0.12$ ($g_2 = 0.12$).

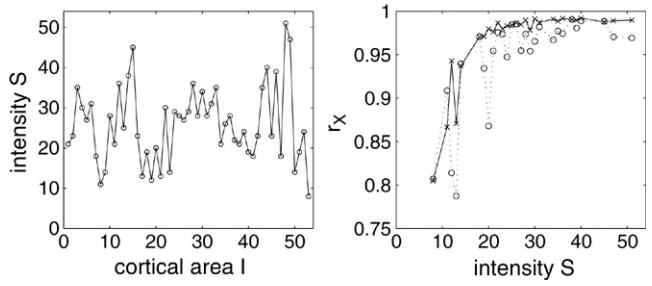

Fig. 12. (a) Input intensity of the areas. (b) The correlation r_X between the local and global mean fields, as a function of the intensity S of the nodes, for the randomized network (solid line) and for the original cat network (dashed line).

dynamics for the mean activity of the sub-networks:

$$\dot{\bar{x}}_I = F(\bar{x}_I) + g_{\text{eff}} \sum_J^N M^R(I, J)(\bar{x}_J - \bar{x}_I), \tag{5}$$

where $F(\bar{x}_I)$ represents the complicated collective dynamics of sub-networks and g_{eff} denotes the effective coupling between the mean activities, both depending on g_1 and g_2. According to our recent analysis in general weighted networks of oscillators [7], when the network is sufficiently random, the input to a node I from its k_I neighbors is already close to the global mean field $X = (1/N)\sum_J^N \bar{x}_J$ if the degree k_I is large enough. Namely, we can take $\sum_J^N M^R(I, J)\bar{x}_J \approx \left[\sum_J^N M^R(I, J)\right] X$ and get the following approximation

$$\dot{\bar{x}}_I = F(\bar{x}_I) + g_{\text{eff}} S_I (X - \bar{x}_I), \qquad k_I \gg 1, \tag{6}$$

where the intensity $S_I = \sum_J^N M^R(I, J)$ is the total of the input weights to the node I. This first-order approximation

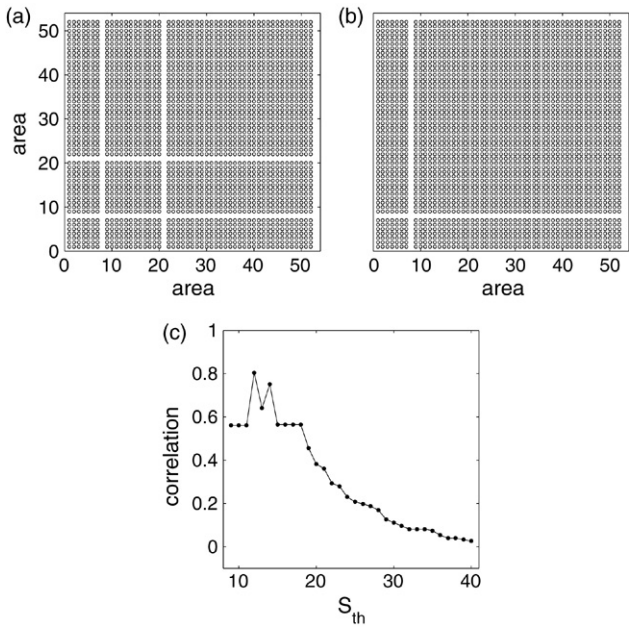

Fig. 13. The relationship between dynamical clustering and node's intensities in random networks. (a) Major dynamical cluster as in Fig. 11 (C_3). (b) Effective cluster C^S defined by Eq. (7) with the threshold $S_{\text{th}} = 12$. (c) The correlation r_C between the dynamical cluster in (a) and the effective cluster C^S, as a function of the threshold S_{th}.

in Eq. (6) means that nodes with large intensities S are more strongly coupled to the global mean field X and synchronize closer to it. The nodes synchronizing commonly with X form an effective cluster, while the nodes with small intensities S are not significantly influenced by the activity of other nodes and preserve their own rather independent dynamics. Comparing the intensities of the nodes in Fig. 12(a) with the clusters in Fig. 11 already provides some evidence for the above argument.

We can compute the correlation between the local mean field $\bar{x}_I$ and the global mean field X, denoted by $r_X(I)$, for each area I. A plot of r_X as a function of the intensity S (taking the average value among the nodes with the same intensity S) is shown in Fig. 12(b). We can see that, for the random network, r_X is an almost monotonously increasing function as we expect from Eq. (6) (except for $S = 11$ corresponding to the node 19 (degree $= 7$) which connects to several neighbors with large intensities in this realization of the random network). From this, we conclude that the major cluster is composed of nodes with intensities S larger than some threshold S_{th}, because these nodes are dynamically close enough to the global mean field X. We obtain such an effective cluster C^S based on the intensities S as

$$C^S(I, J) = \begin{cases} 1 & \text{if } S_I \geq S_{\text{th}} \text{ and } S_J \geq S_{\text{th}}; \\ 0 & \text{otherwise.} \end{cases} \tag{7}$$

A suitable value of the threshold S_{th} can be obtained by examining the correlation r_C between the matrix of the dynamical cluster C_3 in Fig. 11 and the matrix of the effective cluster C^S defined in Eq. (7). The relationship of this correlation coefficient r_C to the threshold value S_{th} is shown in Fig. 13(c). The matrix C^S corresponding to the maximal correlation r_C at $S_{\text{th}} = 12$ is shown in Fig. 13(b). We can

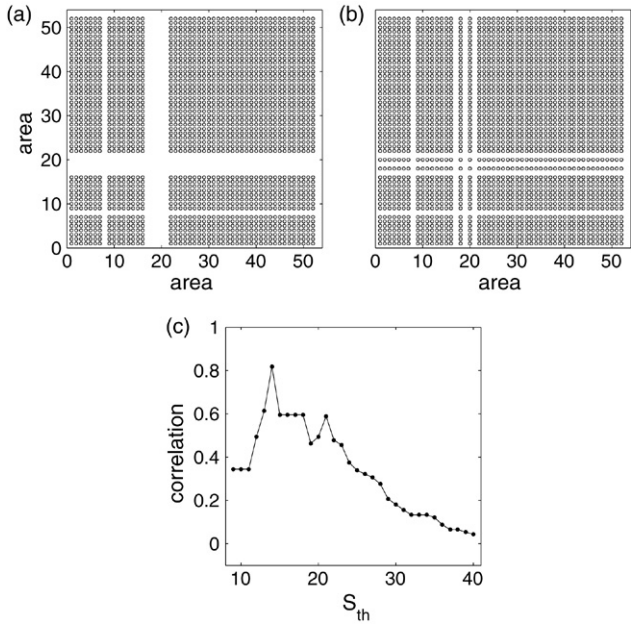

Fig. 14. As in Fig. 13, but for the original cat cortical network. (a) Major dynamical cluster as in Fig. 10 (C_3). (b) Effective cluster C^S defined by Eq. (7) with the threshold $S_{th} = 14$. (c) The correlation r_C between the dynamical cluster in (a) and the effective cluster C^S, as a function of the threshold S_{th}.

see that it differs from the dynamical cluster (plotted again in Fig. 13(a)) only by a single area $I = 21$ in this realization of the random network. The area 21 has an intensity $S = 13$ just beyond the threshold S_{th} and the dynamics is marginal to the major cluster. The other two areas $I = 8$ and $I = 53$ having intensities smaller than the threshold S_{th} are considered as independent clusters, which is also consistent with the observation directly from the dynamical pattern.

Now we perform the same analysis for the original cat cortical network. The correlation r_X between the local mean field $\bar{x}_I$ and global mean field X displays a similar trend as the random networks. The lowest correlation corresponds to the area $I = 53$ (Hippocampus) from the FL system with the minimal intensity $S = 8$. However, there are several areas with intermediate intensities $S \sim 12$–13 and $S \sim 20$, but with significantly lower correlation. These are the areas $I = 19, 17, 21, 20$ (AAF, AI, VPc, P) belonging to the auditory system which form another dynamical cluster (Fig. 9 (C_2)). The effective cluster C^S obtained by thresholding the intensities with the optimal value $S_{th} = 14$ is shown in Fig. 14(b). Apart from a few nodes ($I = 18, 20$) from the auditory system, the argument based on intensities also explains the major dynamical organization in the system.

The above comparison shows that when the coupling is large and synchronization is strong, the organization of the systems into topological communities may not generate corresponding dynamical specialization. The communities having significant inter-community interactions (V, SF and ML) will merge to form a single cluster. The nodes having low connectivity to the rest of the network stay relatively independent, and the dynamical organization is mainly controlled by the intensities, regardless of the network topology.

6. Conclusion and discussion

One of the major challenges in neuroscience as well as in other fields of complex systems is understanding the relationship between the function and the underlying structure of systems. The synchronization dynamics of complex networks can be used to investigate this problem, since synchronization bridges the structure and the function of various systems, including neural systems. We have studied in this paper the relationship between topological structures and synchronization dynamics of neural networks using a realistic network of corticocortical connectivity of cat. With a simplified network model and generic spiking dynamics for the simulation of the otherwise biologically complicated structure and dynamics of each cortical area, we have observed interesting dynamical organization. In the biologically plausible regime of weak synchronization, we have demonstrated a close correspondence between the topological communities and the dynamical clusters. In the light that structure determines dynamics and dynamics controls function, our results provide an explanation from the viewpoint of network dynamics for the coincidence between the topological communities and the functional sub-division in the brain cortex [17,18]. The areas important for inter-community communication and information integration were seen to act as bridges between different topological communities and dynamical clusters. These areas are the same as those previously found to be crucial for the global functioning of the system, as identified in previous studies [12].

We have shown that the relationship between structure and function varies in different dynamical regimes. In the region of large couplings and strong synchronization, the organization of the network into communities does not always separate the dynamics into corresponding clusters. This case corresponds to abnormal synchronous activity of large neuronal assembles, for example, during epileptic seizures. The failure to form different dynamical (functional) clusters indicates the failure to perform distinct functional tasks in different functional sub-systems of the cortex during such pathological events, as is intuitively consistent with experimental observation.

Our modeling and simulation can be extended and improved in several ways, in order to address more realistic information processing in the brain. In our present implementation, the model displays a large region of frequent and regular spiking in the neurons and strong synchronization even without strong external influence. This situation is closer to the epileptic type of abnormal activity [29]. In normal brain, the neurons usually do not exhibit such large activity, and fire for a relatively short time only in the presence of strong enough stimuli from other neurons [32]. Thus, a plausible extension is to implement the sub-network with biologically balanced states, i.e., by considering synaptic interaction (pulse-coupling) and stronger synapses for inhibitory neurons like in balanced networks [33,34].

The interesting clustering dynamics, especially in the biologically plausible regime of weak synchronization, originates from our modeling of the node of the cortical networks with a sub-network of excitable/spiking elements.

Other generic models of excitable/spiking neurons, such as the simple integrate-and-fire (I&F) model, would generate similar results reported in this paper, especially on the systems level. However, cortical neurons display rich dynamics which would require more subtle neuron models to be simulated. Furthermore, biologically, a system of 10^5 neurons corresponding to a cubic millimeter of cortex is the minimal system size at which the complexity of the cortex can be represented, e.g., the number of synapses a neuron receives is 10^4 [35]. Such large sub-networks and other biologically realistic features, such as more detailed spatial structure of neural circuits, seem to be important for the modeling and simulation of experimentally observed hierarchical activity characterized by synchronization phenomena over a wide range of spatial and temporal scales. We are exploring parallel computation for the simulation of such more realistic large-scale neural network models. Another possibility is to model each node of our sub-network by another population of neurons and to employ neural mass models [36] for the node dynamics. The biologically based neural mass models are complicated oscillators describing the mean activities of the neural populations and can reproduce all frequency ranges observed in brain dynamics under different physiological states [36]. In addition, thalamo-cortical connectivity [12] can also be taken into account. With such meaningful extensions, our model could be used to study stimulus evoked brain activities and information processing, and the model dynamics then could be compared to the observed activity spread in cortex [13,37,38] and to the functional connectivity [19–22] at suitable spatio-temporal scales. The analysis and modeling based on the approaches of dynamical complex networks thus can help to obtain a better understanding of the interplay between structures and functions of the neural systems.

Our findings are also interesting in the general aspects of network dynamics. Previous analysis of synchronization dynamics has mainly focused on the stability of ideal case of the complete synchronization state as a function of the global statistics of the networks, such as the mean degree, or the ratio of maximal and minimal eigenvalues, etc. [6–8]. Here we have shown that the detailed dynamical organization varies in different dynamical regimes, determined by different underlying topological structures of the same network (e.g., more local feature of communities, or more global measure of intensities). Other mechanisms of cluster formation in sparsely connected networks have been also reported [39]. Our study reveals both the possibilities and the limitations of the complex network approach for the understanding of complex systems based on the interaction topology. The results also provide an additional motivation to characterize complex network systems beyond global statistics, since more local or detailed connection structures can be the most important determinants for the dynamical behavior of the system. Significant recent interests in this direction are the detection of communities in realistic networks [24,40]. We suggest that the definition of what a community is may have to include the dynamical characterization beyond the topological measures of the systems.

Acknowledgements

The authors thank Claus C. Hilgetag, Gorka Zamora, and James Ong for helpful discussion. This work was supported by the Helmholtz Center for Mind and Brain Dynamics and the DFG Forschungsgruppe “Conflicting Rules”. We acknowledge the Max Planck Institut für Physik Komplexer System for support during the Workshop on “Dynamics on Complex Networks”.

References

[1] R. Albert, A.-L. Barabási, Statistical mechanics of complex networks, Rev. Modern Phys. 74 (2002) 47–97.
[2] S.H. Strogatz, Exploring complex networks, Nature 410 (2001) 268–276.
[3] D.J. Watts, S.H. Strogatz, Collective dynamics of ‘small-world’ networks, Nature 393 (1998) 440–442.
[4] S. Boccaletti, V. Latora, Y. Moreno, M. Chavez, D.-U. Hwang, Complex networks: Structure and dynamics, Phys. Rep. 424 (2006) 175–308.
[5] R. Milo, S. Shen-Orr, S. Itzkovitz, N. Kashtan, D. Chlkovskii, U. Alon, Network motifs: Simple building blocks of complex networks, Science 298 (2002) 824–827.
[6] M. Barahona, L.M. Pecora, Synchronization in small-world systems, Phys. Rev. Lett. 89 (2002) 054101;
T. Nishikawa, A.E. Motter, Y.-C. Lai, F.C. Hoppensteadt, Heterogeneity in oscillator networks: are smaller world easier to synchronize? Phys. Rev. Lett. 91 (2003) 014101;
A.E. Motter, C.S. Zhou, J. Kurths, Enhancing complex-network synchronization, Europhys. Lett. 69 (2005) 334–340;
A.E. Motter, C.S. Zhou, J. Kurths, Network synchronization, diffusion, and the paradox of heterogeneity, Phys. Rev. E 71 (2005) 016116;
M. Chavez, D.-U. Hwang, A. Amann, H.G.E. Hentschel, S. Boccaletti, Synchronization is enhanced in weighted complex networks, Phys. Rev. Lett. 94 (2005) 218701.
[7] C.S. Zhou, A.E. Motter, J. Kurths, Universality in the synchronization of weighted random networks, Phys. Rev. Lett. 96 (2006) 034101;
C.S. Zhou, J. Kurths, Dynamical weights and enhanced synchronization in adaptive complex networks, Phys. Rev. Lett. 96 (2006) 164102.
[8] M. Timme, F. Wolf, T. Geisel, Coexistence of regular and irregular dynamics in complex networks of pulse-coupled oscillators, Phys. Rev. Lett. 89 (2002) 258701;
I. Belykh, E. de Lange, M. Hasler, Synchronization of bursting neurons: What matters in the network topology, Phys. Rev. Lett. 94 (2005) 188101.
[9] L.F. Lago-Fernández, R. Huerta, F. Corbacho, J.A. Sigüenza, Fast response and temporal coherent oscillations in small-world networks, Phys. Rev. Lett. 84 (2000) 2758–2761.
[10] N. Masuda, K. Aihara, Global and local synchrony of coupled neurons in small-world networks, Biol. Cybern. 90 (2004) 302–309.
[11] X. Guardiola, A. Díaz-Guilera, M. Llas, C.J. Pérez, Synchronization, diversity, and topology of networks of integrate and fire oscillators, Phys. Rev. E 62 (2000) 5565–5570.
[12] J.W. Scannell, G.A.P.C. Burns, C.C. Hilgetag, M.A. O’Neill, M.P. Young, The connectional organization of the cortico-thalamic system of the cat, Cereb. Cortex 9 (1999) 277–299.
[13] R. Kötter, F.T. Sommer, Global relationship between anatomical connectivity and activity propagation in the cerebral cortex, Phil. Trans. R. Soc. Lond. B 355 (2000) 127–134.
[14] O. Sporns, G. Tononi, R. Kötter, The human connectome: A structural description of the human brain, PLoS Comput. Biol. 1 (4) (2005) 0245–0251.
[15] O. Sporns, J.D. Zwi, The small world of the cerebral cortex, Neuroinformatics 2 (2004) 145–162.
[16] O. Sporns, D.R. Chialvo, M. Kaiser, C.C. Hilgetag, Organization, development and function of complex brain networks, Trends Cogn. Sci. 8 (2004) 418–425.

[17] C.C. Hilgetag, G.A.P.C. Burns, M.A. O'Neill, J.W. Scannell, M.P. Young, Anatomical connectivity defines the organization of clusters of cortical areas in macaque monkey and cat, Phil. Trans. R. Soc. Lond. B 355 (2000) 91–110.
[18] C.C. Hilgetag, M. Kaiser, Clustered organization of cortical connectivity, Neuroinformatics 2 (2004) 353–360.
[19] C.J. Stam, Functional connectivity patterns of human magnetoencephalographic recordings: A 'small-world' network? Neurosci. Lett. 355 (2004) 25–28.
[20] C.J. Stam, E.A. de Bruin, Scale-free dynamics of global functional connectivity in the human brain, Hum. Brain Mapp. 22 (2004) 97–109.
[21] V.M. Eguíluz, D.R. Chialvo, G. Cecchi, M. Baliki, A. Vania Apkarian, Scale-free brain functional networks, Phys. Rev. Lett. 94 (2005) 018102.
[22] R. Salvador, J. Suckling, M.R. Coleman, J.D. Pickard, D. Menon, E. Bullmore, Neurophysiological architecture of functional magnetic resonance images of human brain, Cereb. Cortex 15 (2005) 1332–1342.
[23] G. Zamora, C.S. Zhou, J. Kurths (unpublished).
[24] M.E.J. Newman, M. Girvan, Finding and evaluating community structure in networks, Phys. Rev. E 69 (2004) 026113;
M.E.J. Newman, Detecting community structure in networks, Eur. Phys. J. B 38 (2004) 321–330.
[25] M.P. Young, The architecture of visual cortex and inferential processes in vision, Spatial Vis. 13 (2000) 137–146.
[26] A.S. Pikovsky, J. Kurths, Coherence resonance in a noise-driven excitable system, Phys. Rev. Lett. 78 (1997) 775–778.
[27] E.M. Izhikevich, Which model to use for cortical spiking neurons? IEEE Trans. Neural Netw. 15 (2004) 1063–1070.
[28] C.S. Zhou, J. Kurths, B. Hu, Array-enhanced coherence resonance: Nontrivial effects of heterogeneity and spatial independence of noise, Phys. Rev. Lett. 87 (2001) 098101.
[29] P. Kudela, P.J. Franaszczuk, G.K. Bergey, Changing excitation and inhibition in simulated neural networks: effects on induced bursting behavior, Biol. Cybern. 88 (2003) 276–285;
K. Lehnertz, C.E. Elger, Can epileptic seizures be predicted? Evidence from nonlinear time series analysis of brain electrical activity, Phys. Rev. Lett. 80 (1998) 5019–5022.
[30] G. Tononi, G.M. Edelman, O. Sporns, Complexity and coherency: Integrating information in the brain, Trends Cogn. Sci. 2 (1998) 474–484.
[31] K.V. Mardia, J.T. Kent, J.M. Bibby, Multivariate Analysis, Academic Press, London, 1989.
[32] E. Niedermeyer, F. Lopes da Silva, Electroencephalography: Basic Principles, Clinical Applications, and Related Fields, Williams & Wilkins, Baltimore, 1993.
[33] C. van Vreeswijk, H. Sompolinsky, Chaos in neuronal networks with balanced excitatory and inhibitory activity, Science 274 (1996) 1724–1726.
[34] N. Brunel, Dynamics of sparsely connected networks of excitatory and inhibitory spiking neurons, J. Comput. Neurosci. 8 (2000) 183–208.
[35] A. Morrison, C. Mehring, T. Geisel, A. Aertsen, M. Diesmann, Advancing the boundaries of high-connectivity network simulation with distributed computing, Neural Comput. 17 (2005) 1776–1801.
[36] O. David, K.J. Friston, A neural mass model for MEG/EEG: Coupling and neuronal dynamics, NeuroImage 20 (2003) 1743–1755.
[37] P.D. MacLean, K.H. Pribram, Neuronographic analysis of medial and basal cerebral cortex I. cat, J. Neurophysiol. 16 (1953) 312–323.
[38] V. Schmitt, R. Kötter, F.T. Sommer, The impact of thalamo-cortical projections on activity spread in cortex, Neurocomputing 52–54 (2003) 919–924.
[39] S. Jalan, R.E. Amritkar, Self-organized and driven phase synchronization in coupled maps, Phys. Rev. Lett. 90 (2003) 014101.
[40] G. Palla, I. Derényi, I. Farkas, T. Vicsek, Uncovering the overlapping community structure of complex networks in nature and society, Nature 435 (2005) 814–818;
L. Danon, A. Díaz-Guilera, J. Duch, A. Arenas, Comparing community structure identification, J. Stat. Mech. (2005) P09008;
A. Arenas, A. Díaz-Guilera, C.J. Pérez-Vicente, Synchronization reveals topological scales in complex networks, Phys. Rev. Lett. 96 (2006) 114102.